ELSEVIER

International Journal of Pharmaceutics 247 (2002) 127–137

international journal of pharmaceutics

www.elsevier.com/locate/ijpharm

Affinity scale between a carrier and a drug in DPI studied by atomic force microscopy

V. Bérard [a,*], E. Lesniewska [b], C. Andrès [a], D. Pertuy [c], C. Laroche [c], Y. Pourcelot [a]

[a] *Pharmacy Division L.P.G., U.F.R. Pharmacy, Université de Bourgogne, F-21079 Dijon, France*
[b] *Physics Laboratory L.P.U.B. UMR CNRS 5027, Université de Bourgogne, F-21078 Dijon, France*
[c] *Pharmaceutical Development GlaxoSmithKline, F-27091 Evreux, France*

Received 20 November 2001; received in revised form 9 July 2002; accepted 17 July 2002

Abstract

The dry powder inhalers (DPIs) consist, in the most cases, of ordered mixture where the particles adhesion results of interactions between the drug and the carrier. Generally, one step of production process is the micronization of the drug particles in order to reduce the size for ordered mixing optimization. But this operation is known to partially create an amorphous surface. In this case, surrounding storage conditions, like relative humidity (RH), are able to modify the percentage of amorphous drug surface. The aim of this study was to investigate surface reactivity, surface energy and direct force measurements by atomic force microscopy (AFM) between lactose (carrier) and zanamivir (drug) crystals references in various conditions of RH. Secondly, an amorphization of the drug surface was induced by humidity relative treatment in order to evaluate the consequences of the transition from crystal to amorphous phase. The study demonstrated that the amorphization of drug surface induces an increase of drug affinity with the carrier surface. Ex situ and in situ amorphization of zanamivir tend to reach the affinity measured between raw materials: carrier and micronized drug particles. AFM allowed adhesion force discrimination between the different forms of the drug particles and demonstrated the potential for investigating adhesion properties in DPI formulation.

Keywords: Dry powder inhaler; Adhesion force; Atomic force microscopy; Relative humidity; Surface amorphization

1. Introduction

In most cases, dry powder inhaler (DPI) formulation consists of small quantities of micronized drug particles (typically less than 1% w/w) mixed with larger carrier particles, ideally forming an ordered blend. The perfect mix consists in a regular coating of fine particles on the coarser constituent. In fact, the quality of the mix directly depends on a dynamic equilibrium between two reversible processes: mixing and segregation. These processes depend on a competition between the adhesion forces existing between the different couples: drug-carrier, carrier–carrier or drug–

* Corresponding author. Tel.: +33-380-393-247; fax: +33-380-393-300
E-mail address: vberard@u-bourgogne.fr (V. Bérard).

0378-5173/02/$ - see front matter
PII: S0378-5173(02)00400-3

drug. Intrinsic factors like the chemical nature of materials, the polymorphism type, and extrinsic factors like the environmental storage conditions influence these forces.

In DPI, the lactose is the most common carrier used for its good lung tolerance. Numerous studies on lactose particles were devoted to investigate the effects of relative humidity (RH), electrostatic charge, and surface characteristics (polymorphism, roughness) on drug-carrier particle interactions and drug release from the carrier. To realise this study, we decided to choose zanamivir as drug. Indeed, zanamivir is representative of a new class of drug developed for the treatment of influenza in respiratory tract (Von Itzstein et al., 1993; Chapple et al., 2000). After chemical synthesis, zanamivir presents a crystalline form. A state of production process is the micronization of zanamivir crystals in order to reduce the particles size for ordered mixing optimization (Staniforth, 1987; Barra et al., 1998; Lucas et al., 1998). The micronization operation is known to partially create an amorphous surface. In addition, surrounding storage conditions are able to modify the percentage of amorphous drug surface. This fact could lead to a modification of the quality of mixing if the amorphous or crystalline drug form does not have the same affinity for the carrier.

The aim of the present work was to quantify the effect of amorphous or crystal transition in order to establish an affinity scale between lactose and the different forms of zanamivir created as references. The affinity can be evaluated by measurement of drug-carrier adhesion force. This particle adhesion force is equivalent in magnitude to the force required for particle detachment. Numerous techniques are available to observe qualitatively adhesion force, including scanning electron microscopy (SEM) ultra-violet (UV) fluorescence microscopy, specific sieve technique, vibration technique, and centrifugation. Recent advances in atomic force microscopy (AFM) have paved the way for force surface investigations (Thundat et al., 1993 Radmacher et al., 1994; Heinz and Hoh, 1999). AFM allows Angström-scale deflections of a probe tip to be measured. Atomic resolution has been obtained, extending micro-contact experiments to the nanometer regime (Baumgartner et al., 2000). The AFM has shown the possibility of directly measuring adhesion force between polymers and flat surface (Biggs and Spinks, 1998) or between various mineral surfaces (Finot et al., 1999, 2000a; Lesko et al., 2001). Experiments have been extended to direct measurement of the colloidal force involved between a silica sphere and carrier particles used in DPI (Louey et al., 2001), or between carrier particles (Sindel and Zimmermann, 2001). In a previous work (Berard et al., 2002), we used AFM to measure the adhesion between lactose compact and crystal zanamivir.

In this study, we first investigated the surface reactivity and the surface energy of carrier and drug particles. Direct force measurements between recrystallized carrier and drug references were performed. An amorphization of the drug surface was then induced in order to evaluate the consequences of the transition from crystal to amorphous phase, and to correlate with adhesion between zanamivir micronized and lactose spray-dried used in DPI.

2. Materials and methods

2.1. Materials

Zanamivir micronized particles were used as supplied by GlaxoSmithKline. The distribution of the particle size of micronized zanamivir was unimodal with a geometric volume mean diameter of 2.5 μm and a geometric standard deviation of 1.5 (Laser scattering, particle suspension in methanol, Coulter LS130, Coultronics, USA). In order to obtain zanamivir crystal reference, zanamivir was recrystallized from a sursaturated solution of micronized drug, after centrifugation, at room temperature (25 °C) in bidistilled water (Milli-Q water, 18.3 MΩ cm, obtained from a Nanopure UV, Barnstead Station, UK). Zanamivir has a solubility of approximately 18 mg/ml in water at 20 °C. The amorphous form reference of zanamivir was obtained ex situ by instantaneous evaporation at 160 °C. In another experiment, we would try to induce an amorphization in situ of zanamivir crystal surface. For that, a zanamivir crystal

was submitted to increase and decrease of RH in cyclical manner. During the RH increase phase from 2 to 85%, crystal surface dissolution should allow to obtain a disorder which should be fixed by a brutal decrease of RH from 85 to 30%. These cycles should be repeated in order to order to increase the surface amorphization of the zanamivir crystal.

Spray-dried lactose was supplied by GlaxoSmithKline (HMS, The Netherlands). Lactose particles presented an unimodal volume diameter distribution with a geometric volume mean diameter typically of 150 μm and a geometric standard deviation of 1.8. In order to minimize the geometric factors and to examine specially the zanamivir form contribution in adhesion, the lactose was 'standardized'. It meant that the spray-dried lactose was recrystallized from a sursaturated lactose solution to obtain a crystal reference. The crystallographic forms were checked by X-Ray diffraction using the CPS-120 INEL Diffraction System fitted with localization curve-Cu anti cathode (120°, 4096 channels). X-Ray analysis revealed the crystallographic form of the recrystallized lactose as alpha-lactose-monohydrate. All crystals and amorphous zanamivir were prepared directly on glass cover slips for AFM studies.

2.2. Methods

The photomicrographs of drug and carrier surfaces sputtered with nickel were taken using SEM (JEOL 6400F, Japan).

AFM measurements were performed using a commercial AFM (Nanoscope IIIa, Veeco Instruments, Santa Barbara, CA). All images were acquired in air using contact mode-AFM (CM-AFM) or oscillating mode (Tapping Mode™ AFM) with the D-type scanner (12 μm) and the J-type scanner (150 μm). For TM-AFM imaging, V-shaped silicon nitride cantilevers with a nominal spring constant of 0.01–0.06 N/m (Thermo Microscopes, Sunnyvale, CA) were used, the other experiments in TM-AFM mode being performed with silicon cantilevers of 20–25 N/m (Veeco Instruments). In order to remove contaminants, the tips were exposed to UV–ozone for 10 min, allowing the removal of the hydrocarbons. For each tip used, the sensitivity response was determined from amplitude calibration plots on glass cover slips. By measuring the resonant frequency of the different cantilevers (with or without fixed particle), the associated spring constant was calculated using Eq. (1) (Cleveland et al., 1993):

$$k = 2(\pi L v)^3 w(\rho^3/E)^{1/2} \quad (1)$$

where L and w represent respectively the length and width of the cantilevers as supplied by the manufacturer, v the resonant frequency, E the Young's modulus, and ρ the density of material of the cantilever.

Force measurements were carried out with Si or Si_3N_4 cantilever (200 μm long) with spring constant k in the range of 0.35–30 N/m. As reference for the discussion, force was evaluated between free AFM probe covered by its thin silicon oxide layer (2–4 nm thick) and the three substrates (zanamivir or lactose crystal and amorphous zanamivir). For particle adhesion measurements, a selected single crystal (with a size range of 5–15 μm long axis) was glued using epoxy glue (Araldite Epoxy Resin) at the free end of the AFM cantilever, which had an inclination of 12°. Care was taken to prevent the spreading of glue around crystal. SEM observations and elemental composition analysis were carried out by energy dispersive spectrophotometry (EDS-Oxford—Inca Energy Software—20 keV) and demonstrated the absence of contaminating glue on the crystal surface facing the substrate.

The force measurements were performed in a cyclical manner (sample extending and retracting). The sample motion rate was fixed at 50 nm/s in such way that the effects of viscosity were avoided (Burnham et al., 1993; Hao et al., 1991). The contact time between particles was estimated to be about 1s. The deflection of the cantilever (perpendicular to the sample surface) due to the force produced by the sample was recorded using both AFM system and an independent recorder (DSP Lock-in amplifier, model SR 850, Stanford Research System, CA). The contact point is defined as the breaking point where the slope of the force versus separation curve, during the tip approach,

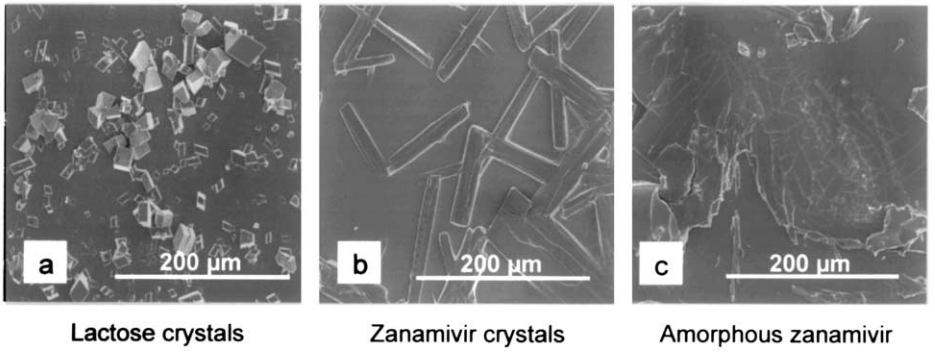

Fig. 1. SEM images (× 300). (a) Lactose crystals. (b) Zanamivir crystals. (c) Amorphous zanamivir prepared ex situ.

changes abruptly. The adhesion force F is calculated according to Hooke's law (Eq. (2)):

$$F = kd \tag{2}$$

where k is the cantilever spring constant and d is the probe–sample separation. Forces versus separation curves were plotted. The adhesion force distribution for each couple was obtained from adhesion measurements realised at nine individual sites and resulting at least from three different experiments.

All AFM studies were carried out under a glass bell jar with controlled atmosphere varying from 2 to 80% RH by step of 10%. A flux of helium gas allowed the work from 2% RH to about 40% RH. The increase of RH from 40 to 80% was achieved by passing decarbonated nitrogen through distilled water. The humidity was measured with an accuracy of 1% with a hygrometer (Quick 74880 Novo Ebro Gmbh, Germany). The temperature under the bell jar was maintained at 25 °C.

3. Results and discussion

3.1. Crystallized and amorphous sample observations

We performed the different techniques of microscopy to evaluate eventual differences in morphology. Using SEM (Fig. 1a), the lactose crystals presented a cube shape of 2–50 µm long. Size of lactose crystals are appropriate for lactose probe preparation. These crystals could be easily manipulated and fixed at the free end of AFM cantilever. Zanamivir crystals presented platelets shape of 100–500 µm long (Fig. 1b). Zanamivir particles were well crystallized with regular plane surfaces particularly in favour of our AFM application. Amorphous zanamivir appeared like plane surface covering the glass substrate (Fig. 1c).

Using AFM, magnifications of × 200 000 revealed enough details of the morphology and surface disorder, as presented in Fig. 2. On several specimens, surface measurements were made using the section analysis module of the AFM software. This module permits the selection of one or more sections of the image and the performance of various measurements, both in horizontal and vertical plane. Surface roughness is defined as the standard deviation of the Z values within the given area and is calculated using Eq. (3):

$$R_q = \sqrt{\frac{\sum (Z_i - Z_{average})^2}{N}} \tag{3}$$

where $Z_{average}$ is the average of the Z values, Z_i is the current Z value and N is the number of points (512×512) within the given area (1 µm^2).

On the lactose surface (Fig. 2a), ridged faces with three-dimensional alignments were observed independently of the scanning direction and the scan rate. In section analysis, the steps were elongated in one direction with variable length and width, and their height ranged from 1.5 to 5 nm. The mean surface roughness over 50 different locations was 1.689 ± 0.361 nm.

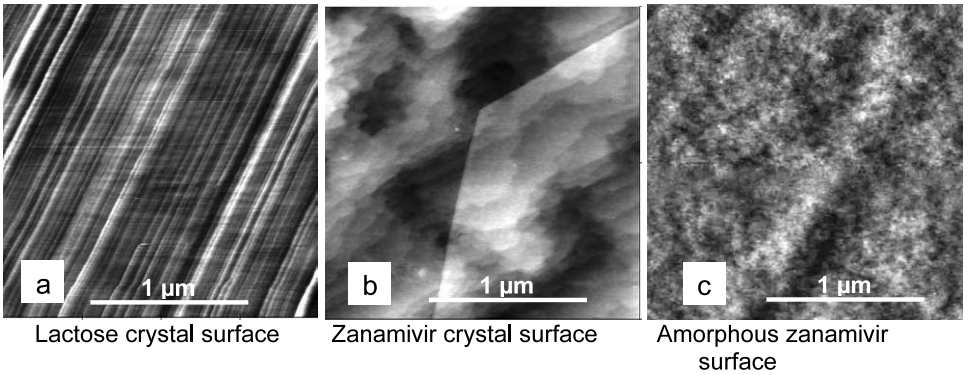

Fig. 2. TM-AFM height images (2×2 µm^2) taken at 35% RH −25 °C. (a) lactose crystalline surface, relative height = 10 nm. (b) Crystalline zanamivir surface, relative height = 20 nm. (c) Amorphous zanamivir surface from sample prepared ex situ, relative height = 3 nm.

On the zanamivir crystal surface (Fig. 2b), terraces were observed. Zanamivir crystals possessed very structured surfaces with remarkable differences in height and extended terraces. Terraces height was a few multiples of the (0 0 1) lattices spacing of zanamivir. The height of the steps between two terraces, measured in section analysis, was 0.89 ± 0.02 nm. The mean surface roughness was estimated to 1.712 ± 0.944 nm.

Zanamivir crystals and amorphous surfaces were clearly distinguishable (Fig. 2c). As expected, the amorphous form had surface smoother without perceptible ordered structures. The mean surface roughness was estimated to 0.445 ± 0.135 nm.

From this topographical information, adhesion force measurements are relevant.

3.2. Capillary forces

Contact forces at different RH were analyzed in order to evaluate the capillary forces existing between the AFM silicon tip and the different specimens. Surfaces were exposed to increasing and decreasing RH between 2 and 80%. Although many humidity experiments were conducted, only results concerning exposure from low to high humidity are presented here. The variations of the contact force, assimilated to the change of the Laplace's pressure, provide information on the quantity of water on the sample and the tip. The model used was previously described more precisely in Finot et al., 1996. Typical force curves are reported in Fig. 3. Retract force curve is connected with the contaminating layer on top of the sample surface (Israelachvili, 1992). On the hydrophilic surface, as the meniscus of water grows between the probe and the sample, the distance required for breaking the meniscus increases. Cantilever with a strong spring constant ($k = 1$–30 N/m) is preferred in order to avoid all frictions and lever torsion at the approach of the surface. This allows the real estimation of the high value of force gradients, and achieves solid–solid contact. In fact, for a cantilever with a high spring constant ($k = 35$ N/m), the distance retract of probe to break the meniscus is about four times the thickness of the contaminating layer covering the surfaces. Whereas in case of more sensitive cantilever ($k = 0.35$ N/m), the retract distance can reach 100 times the thickness of water because of friction (Yoshizawa et al., 1993; Warmack et al., 1994). The very sensitive cantilever, presenting hysteresis of force curves, cannot be used to quantitatively measure the adhesion. Analysis on numerous lactose and zanamivir samples indicated a dependence on both contact point and spring constant of the AFM cantilever. The uncertainty on the contact area limited by the tilt (12°) of the crystal probe, and the spring constant of the cantilever, give the force value with a precision over-estimated to 5%. No influence of the contact duration was observed for all experiments. To check this point, the probe and sample were laid in contact for a set time (1–30 min) with a pressure that did not exceed 100 nN

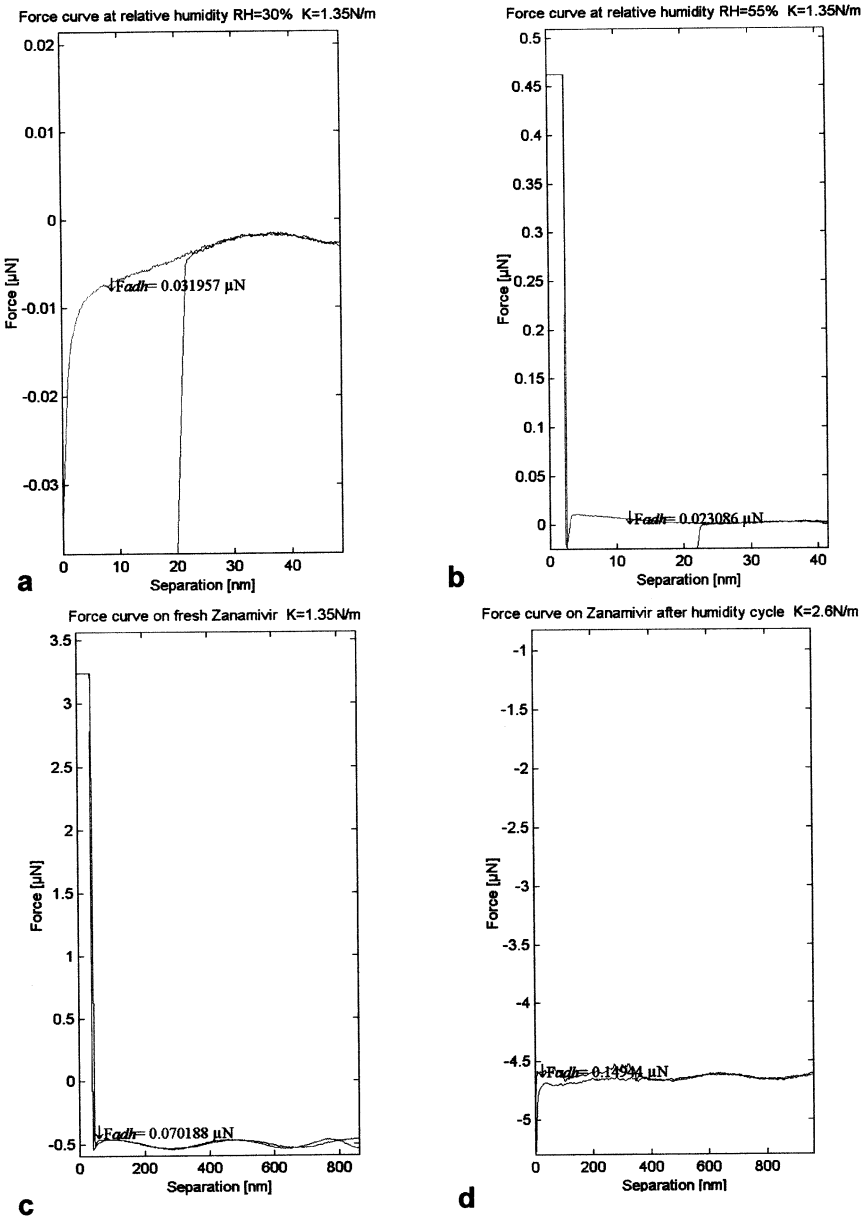

Fig. 3. Illustrations of AFM force versus separation curve. (a) Between AFM SiO_2 tip and crystalline zanamivir at RH = 30% where pure adhesion is noticed ($F_{adh} = 31.96$ nN). (b) Between AFM SiO_2 tip and crystalline zanamivir at RH = 55% where a repulsion force is detected at the approach ($F_{rep} = 2.15$ nN). (c) Between lactose and a crystalline zanamivir at RH = 40% where the adhesion force detected ($F_{adh} = 70.19$ nN) is less than the adhesion force detected ($F_{adh} = 149.44$ nN−RH = 40%) on zanamivir after six humidity cycles (d).

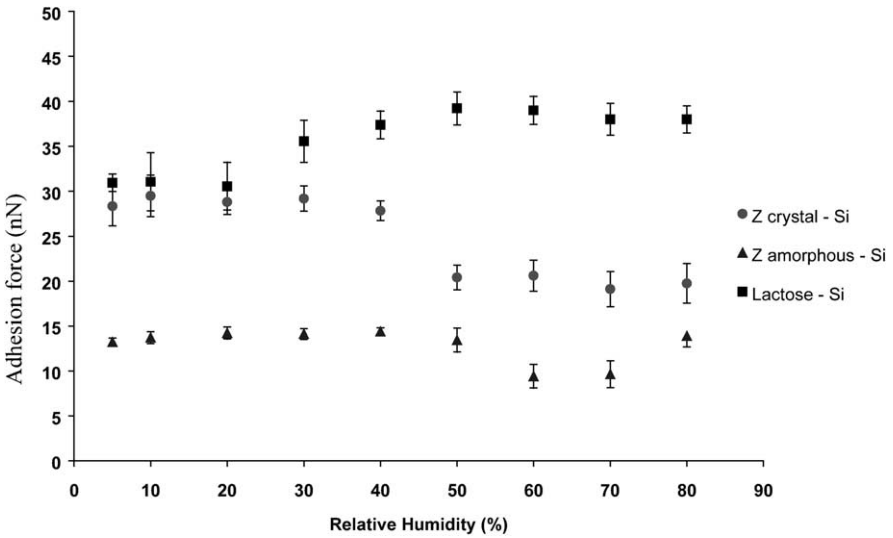

Fig. 4. Comparison of adhesion forces between the AFM tip (SiO_2) and lactose, crystalline zanamivir, and amorphous zanamivir surfaces versus RH.

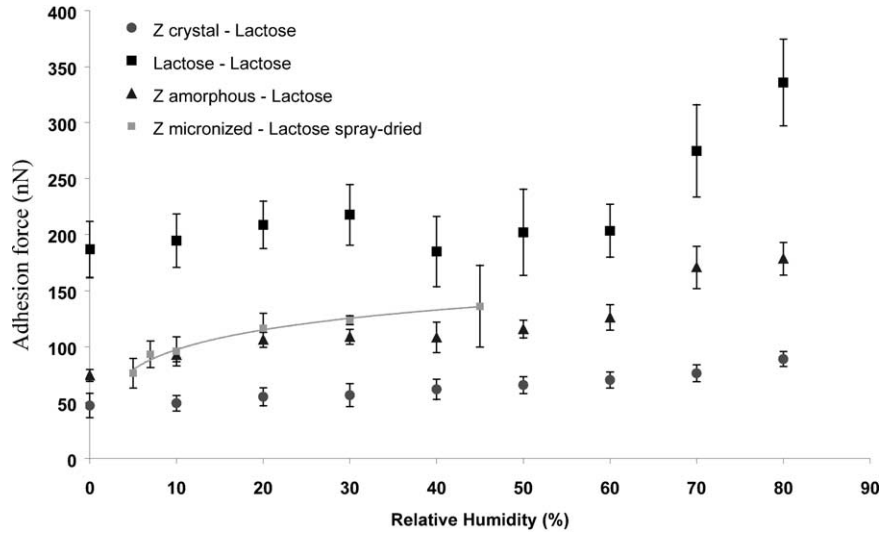

Fig. 5. Comparison of adhesion forces between the lactose crystal fixed on the AFM tip and lactose, zanamivir crystal and amorphous zanamivir surfaces, versus RH. The dashed curve represents the adhesion forces between a particle of micronized zanamivir and a particle of lactose.

(feedback of AFM controller released). Only the first retraction curve of the cantilever deflection was then stored. All collected data presented will concern the force recorded at instantaneous contact. A typical interaction force curves during approach and retraction is shown in Fig. 3a for a zanamivir crystal and the AFM tip contact at 30% RH. The results are very reproducible and the

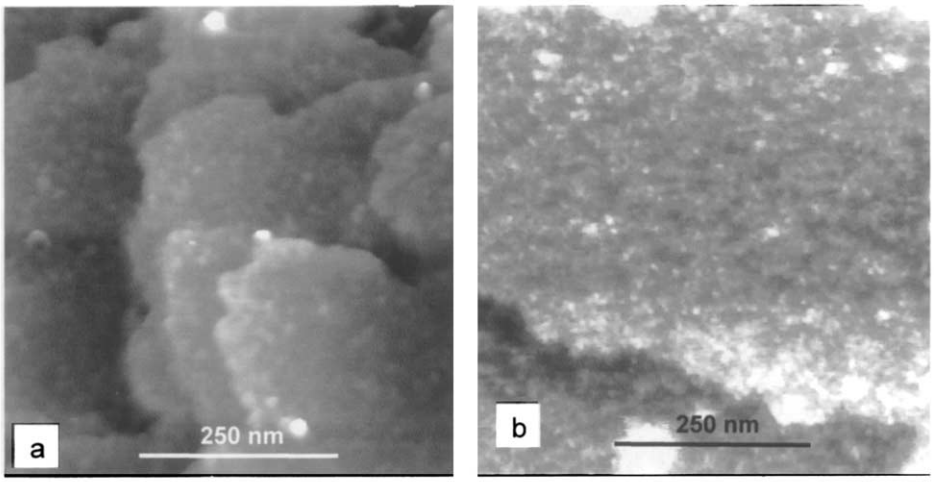

Fig. 6. TM-AFM height images (500 × 500 μm^2) from crystalline zanamivir crystal (a) before humidity relative cycle, relative height = 3 nm. (b) after six cycles, relative height = 2 nm.

same response is found up to a RH of 30%. There is no hysteresis in the attractive regime during retraction. This suggests that there is no meniscus formation as expected for low humidity. Above 45% RH, repulsive force is seen during the approach. Fig. 3b shows the interaction stiffness curve when the RH is 65%. The resulting attractive force is decreased, inconsistent with meniscus formation up to 35% RH. After exposing the specimen to 80% RH, the humidity is reduced. Reducing the humidity back to 2% RH provided similar response observed in the start experiment. The effect to humidity exposure is reversible for zanamivir.

The evolution of adhesion forces facing the AFM tip is described in Fig. 4 (summary of all the experimental data). For zanamivir surfaces, when the RH is increased above 10%, all curves have shown qualitatively the same evolution. Between 10 and 30% RH, all contact forces presented a slight variation of about 1 nN. From 35% RH onwards up to 60%, an abrupt decrease occurred for the adhesion forces concerning all zanamivir-studied surfaces. These results suggest the hydrophobic tendency of zanamivir surfaces. It should be noticed that the surface often has specific properties that are distinct from those of the bulk material.

For lactose, at low RH (0–30%), adhesion forces did not change (Fig. 4). But contrary to the zanamivir surfaces, an increase of adhesion forces occurred above 35% RH, confirming the hydrophilic nature of lactose. These observations are similar to the results presented in the literature using AFM (Binggeli and Mate, 1994; Hu et al., 1995). The effect of humidity exposure was irreversible for lactose. The adhesion forces were

Table 1
Comparison of the adhesion force results obtained with the different configurations

Substrate	AFM probe	
	SiO_2	Lactose
Lactose	31 $nN_{RH=5\%} \rightarrow 39$ $nN_{RH=70\%}$	187 $nN_{RH=5\%} \rightarrow 275$ $nN_{RH=70\%}$
Zanamivir crystal	29 $nN_{RH=5\%} \rightarrow 19$ $nN_{RH=70\%}$	47 $nN_{RH=5\%} \rightarrow 76$ $nN_{RH=70\%}$
Amorphous Zanamivir	13.5 $nN_{RH=5\%} \rightarrow 10$ $nN_{RH=70\%}$	75 $nN_{RH=5\%} \rightarrow 171$ $nN_{RH=70\%}$

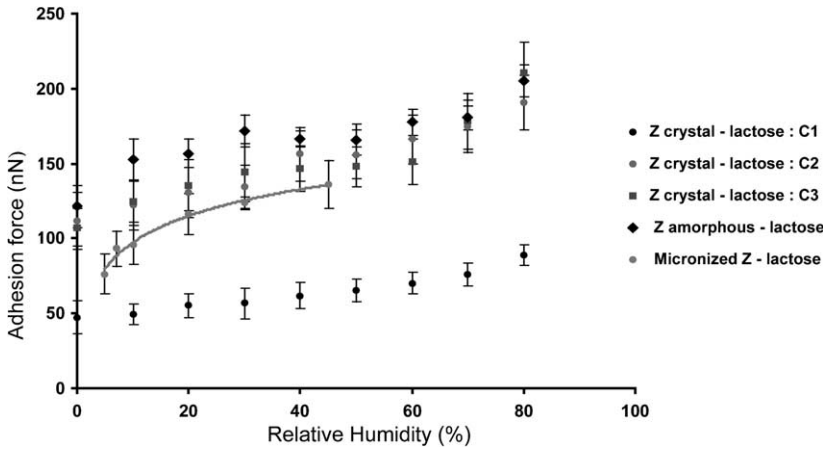

Fig. 7. Evolution of adhesion forces between the lactose crystal fixed on the AFM lever and crystalline zanamivir crystal: amorphization induced in situ by six humidity relative cycles (from C1 to C6) and comparison with adhesion forces between lactose crystal and amorphous zanamivir amorphous produced ex situ. Comparison with results on micronized zanamivir (dashed line).

modified when water adsorption–desorption cycles were performed. The capillary force can be calculated from the subtraction of the force measured at RH lower than 10% to the force measured at RH higher than 35%. The lactose has a capillary force of about 8 nN.

Experimentally, the adhesion energy Γ can be extract from the attractive force F_{adh} using Eq. (4):

$$\Gamma = F_{adh}/(4\pi R_{tip}) \quad (4)$$

where $R_{tip} = 20$ mn represents the AFM tip radius (Finot et al., 1996). Lactose ($F = 31$ nN, $\Gamma = 123$ mJ/m^2) and crystalline zanamivir ($F = 29$ nN, $\Gamma = 115$ mJ/m^2) have surface energies much higher than that of amorphous zanamivir ($F = 13.5$ nN, $\Gamma = 54$ mJ/m^2). In this case, the amorphization decreases the surface energy of zanamivir particles. The adhesion forces measured with the AFM SiO_2 tip presented significant differences with the three materials and followed the order given:

$$F_{\text{zanamivir amorphous}} < F_{\text{zanamivir crystal}} < F_{\text{lactose crystal}}$$

These first results have shown that the two drug phases (i.e. amorphous or crystals) did not create the same force field and could play an important role in adhesion process.

3.3. Adhesion affinity scale

Force measurements between zanamivir and lactose surfaces were conducted under controlled atmosphere.

Due to the surface roughness and the cantilever inclination, the real contact area represents a fraction of the apparent (macroscopic) contact area. The contact area (~ 10 nm^2) has been estimated for each crystal–probe at the end of force measurements by scanning over AFM calibrated grid and using the AFM software for tip shape characterisation. Moreover, the morphologies and the mutual crystal orientation influence the nature of the results. The experiments have shown that there are peaks in the adhesion energy at lattice coincidence angles. The adhesion will be much lower than the maximum theoretical value.

When the AFM probe was replaced by lactose crystal, all adhesion forces were stronger than previously (Fig. 5). The error bars are significant of the differences in adhesion observed between individual sites and samples.

The results of data evaluation are summarised in Table 1.

Two types of remark can be distinguishable. In the first case, the hierarchy observed previously with the SiO_2 tip was modified with the lactose tip.

In the second case, lactose crystals presented the stronger affinity for itself than for zanamivir in the range of 2–80% RH. With the lactose probe, the adhesion force followed the given order:

$$F_{\text{zanamivir crystal}} < F_{\text{zanamivir amorphous}} < F_{\text{lactose crystal}}$$

In this study, we have shown that amorphous zanamivir created ex situ presented stronger adhesion forces with lactose than crystalline zanamivir. As mentioned in introduction, the micronization operation partially creates an amorphous surface and increases the adhesion force between zanamivir and lactose. This fact was pointed out with direct measurements between micronized zanamivir and lactose spray-dried for a range of RH from 2 to 45% (dashed curve on Figs. 5 and 7). Above 45% RH, micronized drug particles came apart from the AFM cantilever.

One objection to these first results might be that particle shape of the zanamivir crystals and amorphous zanamivir created ex situ were different and could modify their affinity hierarchy with lactose. To shake off this possible factor, we realised a succession of humidity relative cycles on the very same crystals of zanamivir in order to perturb its surface structure. It should be noticed that until now no evolution of surface topography has been observed with the tip sweep and the variation in humidity (Finot et al., 2000b). The Fig. 6 presents TM-AFM images of this crystalline zanamivir surface before (Fig. 6a) and after (Fig. 6b) humidity cycles (2–80% RH). We could see that the terraces of the zanamivir crystalline form were covered with non-structured materials constituting typically the amorphous zanamivir form. For each cycle, adhesion force measurements between the zanamivir surface and the lactose probes were realised and the results are presented in Fig. 7. During the first cycle realised on an initial zanamivir crystal, the adhesion forces varied from 50 nN at 0% RH to 80 nN at 80% RH. After each cycle, i.e. in the same time of surface amorphization, we pointed out a systematically increase of these forces (Fig. 3c and d). This increase reached the force values obtained with amorphous zanamivir created ex situ varying from 120 nN at 0% RH to 190 nN at 80% RH. A surface phase transition of zanamivir, independently of particle shape, induced a modification of its affinity for lactose. A process, which led to phase transition, even limited to the surface and possibly no detectable by X-Ray techniques, could produce as a consequence in quality of ordered mix. In this context, we better understand the importance of surrounding storage conditions of DPI.

4. Conclusion

To study the drug adhesion in relation to surface properties in DPIs, AFM was used under controlled atmosphere from 0 to 80% RH.

In a first approach, the characterisation of adhesion properties of AFM silica tip with the carrier and the drug surfaces demonstrates the suitability of AFM to determine the hydrophobic or hydrophilic nature of the surfaces. The ability to generate model surfaces whose structure is controlled on an atomic scale is crucial to obtain a more general understanding of the physics and chemistry of complex surfaces and interfaces.

In a second approach, direct measurements of adhesion between carrier particles and drug surfaces were performed. The adhesion gradually increased with the increasing RH. The amorphization of drug surface induced an increase of the affinity with carrier surface. ex situ and in situ amorphization of zanamivir tends to reach the affinity measured between carrier particles. The micronized drug particles have the same behaviour as amorphous drug. This result, together with morphological data uptake, showed a gradual process of amorphization of the surface. This technique allowed adhesion force discrimination between the different forms of the drug particles and demonstrated the potential for investigating the adhesion properties in DPI formulation.

Acknowledgements

This research was sponsored by GlaxoSmithKline, Department of Pharmaceutical Development Evreux, the CNRS and the Région Bourgogne.

References

Barra, J., Lescure, F., Falson-Rieg, F., Doelker, E., 1998. Can the organization of a binary mix be predicted from the surface energy, cohesion parameter and particle size of its components? Pharm. Res. 15, 1727–1736.

Baumgartner, W., Hinterdorfer, P., Schindler, H., 2000. Data analysis of interaction forces measured with the atomic force microscope. Ultramicroscopy 82, 85–95.

Berard, V., Lesniewska, E., Andres, C., Pertuy, D., Laroche, C., Pourcelot, Y., 2002. Dry powder inhaler: influence of humidity on topology and adhesion studied by AFM. Int. J. Pharm. 232, 213–224.

Biggs, S., Spinks, G., 1998. Atomic force microscopy investigation of the adhesion between a single polymer sphere and a flat surface. J. Adhesion Sci. Technol. 12, 461–478.

Binggeli, M., Mate, C.M., 1994. Influence of capillary condensation of water on nanotribology studied by force microscopy. Appl. Phys. Lett. 65, 415–417.

Burnham, N.A., Colton, R.J., Pollock, H.M., 1993. Interpretation of force curves in force microscopy. Nanotechnology 4, 64–80.

Chapple, K.J., Hendrick, A.E., McCarthy, M.W., 2000. Zanamivir in the treatment and prevention of influenza. Ann. Pharmacother. 34, 798–801.

Cleveland, J.P., Manne, S., Bocek, D., Hansma, P.K., 1993. A non-destructive method for determining the spring constant of cantilevers for scanning force microscopy. Rev. Sci. Instrum. 64, 403–405.

Finot, E., Lesniewska, E., Mutin, J.C., Hosain, S.I., Goudonnet, J.P., 1996. Contact force dependence on relative humidity: investigations using atomic force microscopy. Scanning Microsc. 10, 697–708.

Finot, E., Lesniewska, E., Mutin, J.C., Goudonnet, J.P., 1999. Investigation of surfaces forces between gypsum crystals in electrolytic solutions using microcantilevers. J. Chem. Phys. 111, 6590–6598.

Finot, E., Lesniewska, E., Mutin, J.C., Goudonnet, J.P., 2000a. Investigation of surface forces between gypsum microcrystals in air using atomic force microscopy. Langmuir 16, 4237–4244.

Finot, E., Lesniewska, E., Mutin, J.C., Goudonnet, J.P., 2000b. Correlation between surface forces and surface reactivity in the setting of plaster by atomic force microscopy. Appl. Surf. Sci. 161, 316–322.

Hao, H.W., Baro, A.M., Saenz, J.J., 1991. Electrostatic and contact forces in force microscopy. J. Vac. Sci. Technol. B9, 1323–1328.

Heinz, W.F., Hoh, J.H., 1999. Spatially resolved force spectroscopy of biological surfaces using atomic force microscope. Nanotechnology 17, 143–150.

Hu, J., Xiao, X.D., Ogletree, D.F., Salmeron, M., 1995. Atomic scale friction and wear of mica. Surf. Sci. 327, 358–370.

Israelachvili, J.N., 1992. Adhesion forces between surfaces in liquids and condensable vapours. Surf. Sci. Rep. 14, 109–159.

Lesko, S., Lesniewska, E., Nonat, A., Mutin, J.C., Goudonnet, J.P., 2001. Investigation by atomic force microscopy of forces at the origin of cement cohesion. Ultramicroscopy 86, 11–21.

Louey, M.D., Mulvaney, P., Stewart, P.J., 2001. Characterisation of adhesional properties of lactose carriers using atomic force microscopy. J. Pharm. Biomed. Anal. 25, 559–567.

Lucas, P., Anderson, K., Staniforth, J.N., 1998. Protein deposition from dry powder inhalers: fine particle multiplets as performance modifiers. Pharm. Res. 15, 562–569.

Radmacher, M., Cleveland, J.P., Fritz, M., Hansma, H.G., Hansma, P.K., 1994. Mapping interaction forces with the atomic force microscope. Biophys. J. 66, 2159–2165.

Sindel, U., Zimmermann, I., 2001. Measurement of interaction forces between individual powder particles using atomic force microscope. Powder Technol. 117, 247–254.

Staniforth, J.N., 1987. Order out of chaos. J. Pharm. Pharmacol. 39, 329–334.

Thundat, T.G., Zheng, X.Y., Chen, G.Y., Sharp, S.L., Warmack, R.J., Schowalter, L.S., 1993. Characterization of atomic force microscopy tips by adhesion force measurements. Appl. Phys. Lett. 63, 2150–2152.

Von Itzstein, M., Wu, W.Y., Kok, G.B., Pegg, M.S., Dyason, J.C., Jin, B., Phan, T.V., Smythe, M.L., White, H.F., Oliver, S.W., Colman, P.M., Varghese, J.N., Ryan, D.M., Woods, J.M., Bethell, R.C., Hotham, V.J., Cameron, J.M., Penn, C.R., 1993. Rational design of potent sialidase-based inhibitors of influenza virus replication. Nature 363, 418–423.

Warmack, R.J., Zheng, X.Y., Thundat, T.G., Allison, D.P., 1994. Frictions effects in the deflection of atomic force microscopy cantilevers. Rev. Sci. Instrum. 65, 394–399.

Yoshizawa, H., Chen, Y.L., Israelachvili, J.N., 1993. Fundamental mechanisms of interfacial friction: 1. Relation between adhesion and friction. J. Phys. Chem. 97, 4128–4140.